

# Pressure dependence of the Boson peak in glasses

V. L. Gurevich

*Solid State Physics Division, A. F. Ioffe Institute, 194021 Saint Petersburg, Russia*

D. A. Parshin

*Saint Petersburg State Polytechnical University, 195251 Saint Petersburg, Russia*

H. R. Schober

*Institut für Festkörperforschung, Forschungszentrum Jülich, D-52425 Jülich, Germany*

(Dated: June 24, 2018)

The inelastic scattering intensities of glasses and amorphous materials has a maximum at a low frequency, the so called Boson peak. Under applied hydrostatic pressure,  $P$ , the Boson peak frequency,  $\omega_b$ , is shifted upwards. We have shown previously that the Boson peak is created as a result of a vibrational instability due to the interaction of harmonic quasi localized vibrations (QLV). Applying pressure one exerts forces on the QLV. These shift the low frequency part of the excess spectrum to higher frequencies. For low pressures we find a shift of the Boson peak linear in  $P$ , whereas for high pressures the shift is  $\propto P^{1/3}$ . Our analytics is supported by simulation. The results are in agreement with the existing experiments.

PACS numbers: 61.43.Fs, 63.50+x, 78.30.Ly

## I. INTRODUCTION

One of the most characteristic properties of glasses is a maximum in the low frequency part of their inelastic scattering intensities.<sup>1</sup> This maximum, the Boson peak (BP), originates from a maximum of the ratio  $g(\omega)/\omega^2$  where  $g(\omega)$  is the density of vibrational states which itself often has no corresponding maximum.<sup>2</sup> The BP shows an excess of low frequency vibrations above the Debye contribution of the sound waves. The BP is observed in experiments on Raman scattering of light and inelastic neutron scattering within the frequency interval 0.5 — 2 THz. It is considered to be one of the universal properties of glasses and is found also in a number of other disordered systems (see Ref. [3] and references therein).

Disorder affects the vibrational states differently than it affects the electronic ones. The main point is that the matrix determining the eigenvalues of the harmonic vibrations, the squared frequencies, must satisfy the requirement of mechanical stability (*cf.* Ref.<sup>4</sup>). In other words, all eigenvalues must be positive, apart from the six zero values for translation and rotation of the system as a whole. Other than in the case of electronic states, there is a fixed zero level. An arbitrary random matrix has no such property. This means that, in general, such a matrix corresponds to an unstable vibrational system. Such a mechanical instability has often been observed in numerical simulations of disordered vibrational systems for sufficiently large degree of disorder (*cf.* Refs. [5,6,7]).

However, stability is restored automatically when the effects of anharmonicity are taken into account.<sup>3</sup> A random matrix with the desired stability property is generated in a natural way by solving the corresponding non-linear problem. It is remarkable that the density of states  $g(\omega)$  of such a "stable matrix" possesses the BP feature. The BP is a reminder of the former mechanical instability

in the system.

For the proper interpretation of the BP, the key problem is the nature of the vibrations that contribute to  $g(\omega)$ . Since the term BP is used for any peak in the low frequency inelastic scattering intensity one has to distinguish between different cases. In some materials the BP is ascribed to low lying optical or transverse acoustic modes of parental crystals<sup>8,9,10</sup> or to librations of some molecules in plastic crystals.<sup>11,12</sup> If these excitations have a small frequency spread they will show as a peak in  $g(\omega)$ . The role of disorder is merely to broaden modes which exist already without disorder. In the opposite case the excess of low frequency modes is caused by disorder itself. A simple example is realised in a metallic like model glass where the parent crystal is fcc.<sup>13</sup> In the present paper we discuss this latter case. Between these two extreme cases of well defined low frequency modes, broadened by disorder, and no such modes before disorder, there is a range of materials having aspects of both. Despite being derived for the case of a disorder-induced BP, our results will apply, at least semi-quantitatively, to these intermediate cases as long as the frequency spread of the relevant low frequency modes is sufficiently large.

Starting point of our investigation are the ubiquitously occurring quasilocal (or resonant) harmonic vibrations (QLV). These vibrations can be understood as a low frequency vibration of a small group of atoms which has a weak bilinear interaction with the continuum of acoustic vibrations of the whole system. They share many properties of the localized vibrations but are different from these exact harmonic eigenstates. They can be seen as resonances in the low frequency part of the local spectra of the set of atoms involved. In Mößbauer experiments one observes anomalously large Debye-Waller factors for the atoms vibrating with such QLV<sup>14</sup>. In simulations the QLV are seen in the harmonic eigenstates as "low

frequency localized modes” or mixed into the extended modes. This is found for the textbook case of a heavy mass defect as well as for QLV in glasses<sup>15</sup>. A “low frequency localized mode” of a small system does not vanish when the system becomes larger – it just hybridizes with the other modes of similar frequency. If one looks at the modes around the QLV-frequency one still finds an additional eigenmode. A more detailed discussion of QLV with emphasis on glasses can be found in our previous work on the Boson peak<sup>3</sup> where one can also find supporting references.

In the soft potential model<sup>16,17</sup> one describes the low frequency vibrations of the defect system in the harmonic approximation utilizing a basis of (extended) sound waves and local oscillators. The latter are the cores of the QLV or “bare QLV” which have been found to extend over several atoms<sup>18,19</sup>. In this basis there is a bilinear interaction which is treated as a perturbation.

## II. EFFECTS OF FINITE CONCENTRATION OF QUASI LOCALIZED VIBRATIONS

In a glass one has a finite concentration of QLV’s. As discussed in our previous paper<sup>3</sup>, this has a profound effect on their density of states (DOS). The interaction of the QLV’s with the sound waves induces an elastic dipole interaction between them. First, the interaction of soft QLV’s with surrounding QLV’s of higher frequency may lead in harmonic approximation to unstable modes. Stability is restored by the anharmonic terms. This leads to a linear density of states,  $g(\omega) \propto \omega$ , for  $\omega < \omega_c$  where  $\omega_c$  is determined by the typical interaction strength.

Secondly, these renormalized low frequency QLV’s interact with each other. In effect this means that the QLV’s are subject to random forces,  $f$ , later referred to as *internal forces*. Due to the high susceptibility of low frequency vibrations their low frequency DOS is changed to  $g(\omega) \propto \omega^4$  for  $\omega < \omega_b$ . This is a general property of the low frequency DOS of non-Goldstone bosonic excitations in random media<sup>4</sup> and has been discussed in numerous papers on low energy excitations in glasses, see Refs. [4,17,18,20,21]. It is associated with the so-called *sea-gull singularity* in the distribution of the stiffness constants of the QLV<sup>17,18</sup> in the soft potential model<sup>17</sup>. This sea-gull singularity has also been observed in computer simulations<sup>22,23</sup>.

By the crossover between the two limiting regimes of the DOS the BP is formed and obtains a “universal” shape. The frequency of the BP,  $\omega_b$ , is again determined by the interaction strength and thus by the characteristic value of the internal forces,  $f_0$  (in Ref. [3] this quantity was denoted as  $\delta f$ ):

$$\omega_b \propto f_0^{1/3}. \quad (1)$$

With higher interaction  $\omega_b$  is shifted upwards and the intensity of the BP is reduced<sup>3</sup>.

One of the most interesting properties of the Boson peak in glasses is its shift towards higher frequencies under application of hydrostatic pressure. In the present paper we will show that such a shift can be visualized as a result of a simple physical mechanism. If one applies a pressure  $P$  onto a specimen of glass the internal random forces acquire additional random contributions  $\Delta f$  proportional to the pressure. As a result, one obtains a “blue” shift of the Boson peak frequency with pressure. For small pressure this pressure contribution is small compared to the characteristic value of internal forces  $f_0$  and the shift of the BP is linear in the pressure. With increasing pressure  $\Delta f$  can become larger than  $f_0$  and the BP shifts as  $\omega_b \propto P^{1/3}$ .

## III. RANDOM FORCE DISTRIBUTION IN A GLASS UNDER PRESSURE

In the present Section we will briefly derive, in analogy to Ref. [3], the random force distribution under an applied hydrostatic pressure. From Hook’s law one gets

$$\varepsilon_{ik} = -(P/3K)\delta_{ik}. \quad (2)$$

where  $\varepsilon_{ik}$  is the strain tensor and  $1/K$  is the compressibility of the glass.

The interaction of a QLV with the strain is bilinear<sup>24</sup>

$$\mathcal{H}_{\text{int}} = \Lambda_{ik}\varepsilon_{ik}x = -(P/3K)\Lambda_{ii}x \quad (3)$$

where  $\Lambda_{ik}$  is the deformation potential tensor and  $x$  is the coordinate of the QLV. For simplicity we will write in the following  $\Lambda$  instead of  $\Lambda_{ii}$ . Thus the additional contribution to the random force due to applied pressure is proportional to the pressure

$$\Delta f = (P/3K)\Lambda. \quad (4)$$

The deformation potential  $\Lambda$  of a QLV is a random quantity. In particular, it has a random sign, so that the corresponding distribution function  $D(\Lambda)$  is an even function of  $\Lambda$ . As a result the distribution of the random forces  $f$  in the glass remains an even function of  $f$  when the pressure is applied.

The total random force  $\tilde{f}$  is a sum of two contributions

$$\tilde{f} = f + \Delta f. \quad (5)$$

Here  $f$  is the internal random force in the absence of pressure. If the distribution of the internal forces  $f$  is  $Q(f)$  then the distribution of the total random force  $\tilde{f}$  in a glass under pressure is given by the convolution

$$F_P(\tilde{f}) = \int_{-\infty}^{\infty} d\Lambda Q\left(\tilde{f} - \frac{\Lambda}{3K}P\right) D(\Lambda). \quad (6)$$

For  $P = 0$  it reduces to the unperturbed distribution  $Q(f)$  since the distribution  $D(\Lambda)$  is normalized to unity.

In the Appendix we give the results of the convolution for three cases which should be typical, namely two types of Lorentzian distributions and a Gaussian distribution of  $f$  and  $\Lambda$ .

#### IV. THE BOSON PEAK SHIFT UNDER PRESSURE

Let us discuss how random forces change the frequencies of the QLV's. In a purely harmonic case, the linear forces would not affect the frequencies. Anharmonicity, however, renormalizes the relevant part of the spectrum<sup>3,17</sup>. Although the QLV's are essentially harmonic vibrations their frequencies under applied forces can be shifted as in the usual quasi-harmonic approximation.

To start the description of a QLV, consider an anharmonic oscillator under the action of a random static force  $\tilde{f}$

$$U(x) = Ax^4/4 + M\omega_1^2 x^2/2 - \tilde{f}x. \quad (7)$$

Here  $\omega_1$  is the oscillator frequency in the harmonic approximation and  $A$  is the constant of anharmonicity. The role of the omitted third order term as well as that of the distribution of  $A$  will be discussed further on. The force  $\tilde{f}$  shifts the equilibrium position from  $x = 0$  to  $x_0 \neq 0$ , given by

$$Ax_0^3 + M\omega_1^2 x_0 - \tilde{f} = 0, \quad (8)$$

where the oscillator has a new *harmonic* frequency

$$\omega_{\text{new}}^2 = \omega_1^2 + 3Ax_0^2/M. \quad (9)$$

If  $\tilde{g}_1(\omega_1)$  is the distribution function of frequencies  $\omega_1$  and  $F_P(\tilde{f})$  is the distribution of random forces in a glass under pressure, then the pressure dependent renormalized DOS is given by

$$g_P(\omega) = \int_0^\infty \tilde{g}_1(\omega_1) d\omega_1 \int_{-\infty}^\infty d\tilde{f} F_P(\tilde{f}) \delta(\omega - \omega_{\text{new}}). \quad (10)$$

Integrating the  $\delta$ -function with regard of Eqs. (8) and (9) we get

$$g_P(\omega) = 2M\sqrt{\frac{M}{3A}}\omega^3 \int_0^\omega \frac{\tilde{g}_1(\omega_1) d\omega_1}{\sqrt{\omega^2 - \omega_1^2}} F_P(f_{\omega, \omega_1}). \quad (11)$$

Here

$$f_{\omega, \omega_1} = \frac{M}{3}\sqrt{\frac{M}{3A}} (\omega^2 + 2\omega_1^2) \sqrt{\omega^2 - \omega_1^2}. \quad (12)$$

As shown in Ref. [3] and shortly discussed in section II the interaction of high and low frequency QLV lead to a linear DOS in the relevant frequency range. In writing Eq. 7 we took QLV already including this effect.

Therefore, we can approximate  $\tilde{g}_1(\omega_1) = C\omega_1$  and write Eq. (11) in the form

$$g_P(\omega) = 2CM\sqrt{\frac{M}{3A}}\omega^4 \int_0^1 \frac{dy y}{\sqrt{1-y^2}} \times F_P \left[ \frac{M}{3}\sqrt{\frac{M}{3A}}\omega^3 (1+2y^2) \sqrt{1-y^2} \right]. \quad (13)$$

Let us introduce a characteristic value  $\tilde{f}_0(P)$  of the total random forces acting on the QLV's under pressure. This is the characteristic scale of variation of the argument of  $F_P(\tilde{f})$ . Depending on the relative strengths of the internal forces without pressure and the pressure induced forces, the following estimates hold

$$\tilde{f}_0(P) \approx \begin{cases} f_0 [1 + \mathcal{O}(P/P_0)] & \text{for } P \ll P_0 \\ (P/P_0)f_0 & \text{for } P \gg P_0. \end{cases} \quad (14)$$

Here  $P_0$  is the characteristic pressure, which in the simple case of Lorentzian distributions centered around 0 (see Eqs. A1, A2), is given by  $P_0 = 3Kf_0/\Lambda_0$ . Thus for  $P \ll P_0$ ,  $\tilde{f}_0(P) = f_0$  while for  $P \gg P_0$ ,  $\tilde{f}_0(P) \propto P$ .

According to Ref. [3], for a Lorentzian distribution of random forces, the Boson peak frequency is given by

$$\omega_b(P) \approx \frac{1.9A^{1/6}\tilde{f}_0^{1/3}(P)}{M^{1/2}}. \quad (15)$$

For frequencies  $\omega \ll \omega_b(P)$  the argument of the function  $F_P$  in Eq. (13) is much smaller than the typical value of  $\tilde{f}_0(P)$ . One can replace this function by  $F_P(0) \approx 1/\tilde{f}_0(P)$ . According to Eq. (13),  $g_P(\omega) \propto F_P(0)\omega^4$ . Thus at high pressures  $P \gg P_0$ ,

$$g_P(\omega) \propto \omega^4/P \quad \text{for } \omega \ll \omega_b(P). \quad (16)$$

In the opposite case  $\omega \gg \omega_b(P)$  the integral over  $y$  is dominated by such values of  $y$  near the upper limit that

$$\sqrt{1-y} \lesssim \frac{1}{M}\sqrt{\frac{A}{M}} \frac{\tilde{f}_0(P)}{\omega^3} \ll 1. \quad (17)$$

After integration, making use of the normalization of  $F_P(\tilde{f})$ , we regain the equation for the unperturbed pressure-independent linear density of states

$$g_P(\omega) = \tilde{g}_1(\omega) \propto \omega \quad \text{for } \omega_b(P) \ll \omega < \omega_c \quad (18)$$

as it should be. For higher  $\omega$  ( $\omega > \omega_c$ ) the linear DOS produced by the interaction between the QLV will be modified and  $g_P(\omega)$  shows material dependent deviations.

Fig. 1 shows the frequency dependence of the BP for different applied pressures. Both the distributions of internal forces  $f$  and of the deformation potentials  $\Lambda$  were approximated by Lorentzians centered at 0. After convolution a broadened Lorentzian is obtained, Eq. (A3). One

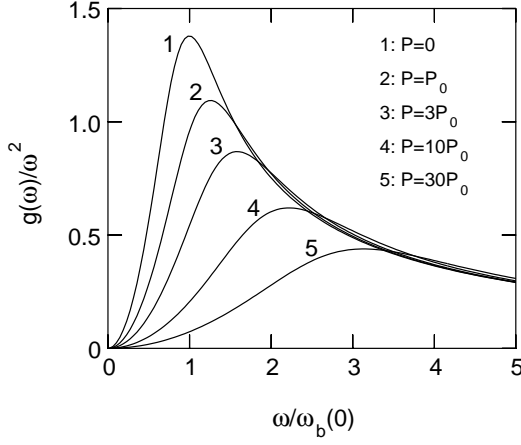


FIG. 1: Boson peak according to Eq. (13) for different applied pressures, excluding the low frequency Debye contribution. Lorentzian distributions were assumed for both internal and pressure induced forces, Eq. (A3).

clearly observes the pronounced flattening with pressure of the low frequency part of the BP. Contrary to this, the high frequency part is not affected. In calculating the curves in Fig. 1 we assumed  $\tilde{g}_1(\omega) \propto \omega$ . In real materials, this linearity of the DOS will only hold up to some frequency  $\omega_c$ . Above that frequency the DOS will be material dependent and, therefore, the BP will no longer have a universal form above that frequency. This can be seen by comparison of the present Fig. 1 with Fig. 3 of Ref. [3].

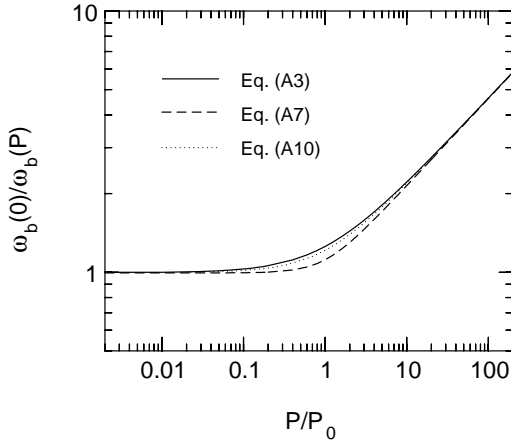


FIG. 2: Frequency  $\omega_b$  of the Boson peak maximum as a function of applied pressure for different force distributions. Solid line: Lorentzian distributions Eq. (A3); dashed line: Gaussian distributions Eq. (A7); dotted line: double Lorentzian distribution, Eq. (A10), with  $\lambda = \sqrt{2}\Lambda_0$ .

The variation of the BP frequency,  $\omega_b$ , with pressure is shown in Fig. 2 for different distributions of the internal forces and deformation potentials. The limiting behavior for small and large pressures is independent of

the distributions. The crossover, on the other hand, does somewhat depend on the type of distribution used. This indicates a material dependence in this pressure range. The shift of  $\omega_b$  with pressure can be described for the Lorentzian distributions, Eq. (A1-A4), by

$$\omega_b(P) = \omega_b(0) \left(1 + \frac{|P|}{P_0}\right)^{1/3} \quad (19)$$

with

$$P_0 = 3K f_0 / \Lambda_0. \quad (20)$$

and for the Gaussian distributions, Eq. (A5-A8), by the slightly different form

$$\omega_b(P) = \omega_b(0) \left(1 + \left(\frac{|P|}{P_0}\right)^2\right)^{1/6} \quad (21)$$

which describes a sharper crossover.

## V. NUMERICAL SIMULATION

### A. Pressure dependence

To test our analytic description we extended the numerical simulations of Ref. [3] to include additional external forces  $\Delta f$ , Eq. (4). We placed  $N = 2197$  oscillators with frequencies  $0 < \omega_i < 1$  on a simple cubic lattice with lattice constant  $a = 1$  and periodic boundary conditions. The bilinear interaction between two oscillators,  $i, j$ , is written as

$$U_{\text{int}}^{ij} = g_{ij} \cdot (J/r_{ij}^3) x_i x_j, \quad (22)$$

where  $r_{ij}$  is the distance between the oscillators and  $J$  is the strength of their coupling which results from the coupling of bare QLV's and sound waves,  $J = \Lambda^2 / \rho v^2$ . Here  $\rho$  is the density and  $v$  the average sound velocity of the material. To simulate random orientations of the oscillators we took for  $g_{ij}$  random numbers in the interval  $[-0.5, 0.5]$ . The masses,  $M_i$ , and anharmonicity parameters,  $A_i$ , were put to 1. The DOS for the noninteracting oscillators was taken as  $g_0(\omega) \propto \omega^n$ , with  $n = 1, 2$ . Random forces

$$\Delta f^i = g_i \cdot f_{\text{ext}}^0 \quad (23)$$

were exerted on the oscillators where  $g_i$  were random numbers in the interval  $[-0.5, 0.5]$ .

Generalizing the potential energy Eq. (7) for one oscillator to the system of  $N$  oscillators and adding the interaction terms described by Eq. (22), we then minimized the potential energy of the total system of  $N$  coupled anharmonic oscillators. In the usual harmonic expansion around this minimum we calculated the DOS for different values of  $f_{\text{ext}}^0$ , representing different external pressures. This was repeated for up to 10000 representations.

The frequency dependence of  $g(\omega)/\omega^2$  is given in Fig. 3, for  $g_0(\omega) \propto \omega$  and  $J = 0.07$ , for different strengths of the external force,  $f_{\text{ext}}^0$ . The behavior of the analytic results, Fig. 1, is reproduced. The slightly different maximal intensities for the higher forces (pressures) result from the different choice of distribution for the external forces (square instead of Lorentzian). The internal forces originate in the simulation directly from the bilinear interaction.

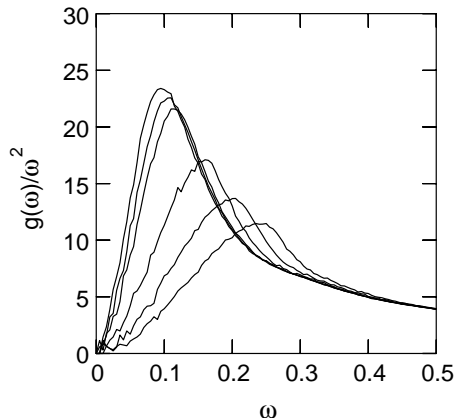


FIG. 3: Simulated  $g(\omega)/\omega^2$  for different external force strengths ( $N = 2197$ ,  $g_0(\omega) \propto \omega$ ,  $J = 0.07$ ). Curves from left to right:  $f_{\text{ext}}^0 = 10^{-4}$ ,  $6 \cdot 10^{-4}$ ,  $10^{-3}$ ,  $3 \cdot 10^{-3}$ ,  $6 \cdot 10^{-3}$  and  $10^{-2}$ .

The pressure dependence of BP frequency is shown in a double logarithmic plot in Fig. 4 for two different original DOS's:  $g_0(\omega) \propto \omega$  and  $g_0(\omega) \propto \omega^2$ . The results for both sets agree with our theoretical predictions. This illustrates that our results are indeed independent of the choice of the initial  $g_0(\omega)$ , as long as it is not too strongly peaked. As stressed in our previous work, above some frequency  $\omega_c$  which is generally well separated above  $\omega_b$ , the redistribution of frequencies becomes ineffective and the original  $g_0(\omega)$  survives. For instance in a plot of  $g(\omega)/\omega^2$ , corresponding to Fig. 3, for  $g_0(\omega) \propto \omega^2$  the curves converge to a constant given by the normalization, and the maximal intensities decay more slowly.

### B. Oscillator participation numbers

In our model the formation of the BP is driven by the interaction between soft oscillators (bare QLV's). At low frequencies this interaction is weak and, therefore, the QLV's will be only weakly coupled. The BP frequency is determined by the typical interaction strength between the oscillators. To quantify the interaction we introduce an oscillator participation number

$$n_{\text{osc}}(\omega) = \left\langle \left( \sum_j |e^j|^4 \right)^{-1} \right\rangle_\omega \quad (24)$$

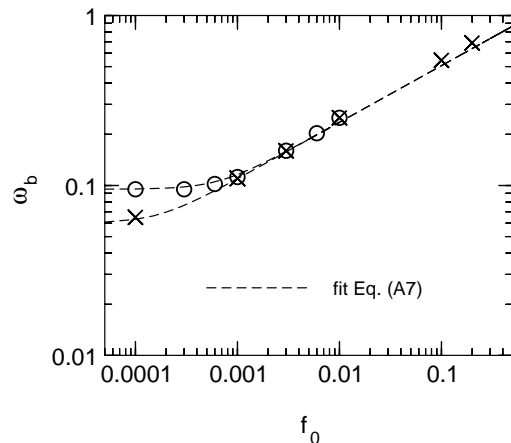


FIG. 4: Boson peak frequency,  $\omega_b$ , versus external force strength on a double logarithmic scale: crosses:  $N = 2197$ ,  $g_0(\omega) \propto \omega^2$ ,  $J = 0.1$ ; circles:  $N = 2197$ ,  $g_0(\omega) \propto \omega$ ,  $J = 0.07$ . The dashed lines give fits with Gaussian force distributions (fit parameters  $\omega_b$  and  $P_0$ ).

where  $e^j$  denotes the component on oscillator  $j$  of an eigenvector of the coupled oscillator system and  $\langle \dots \rangle_\omega$  indicates the average over all eigenmodes of frequency  $\omega$ . Note that this oscillator participation number is different from the usual (atomic or molecular) participation number of an eigenmode of an atomic system. First a QLV (an oscillator in the present description) has typically an atomic participation number of ten or more<sup>18,19</sup>. An oscillator participation number of ten is then equivalent to an atomic participation number of a hundred or more. Secondly the participation numbers are further increased by the interaction between the QLV's and the sound waves<sup>15</sup>. Here this hybridisation is only included in so far as it brings about the interaction between QLV's.

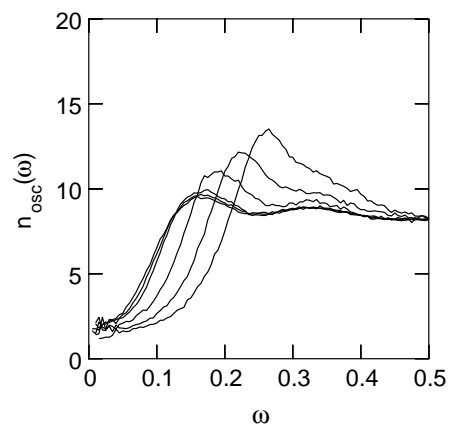


FIG. 5: Average oscillator participation numbers as function of frequency for different external force strength. The curves correspond to the systems of Fig. 3.

For all values of the applied external force,  $f_{\text{ext}}^0$ ,  $n_{\text{osc}}(\omega)$

shows in Fig. 5 the same qualitative behavior as function of  $\omega$ . For small frequencies, one has more or less isolated QLV's ( $n_{\text{osc}}(\omega) \approx 2$ ). With increasing frequencies, coupling and hence  $n_{\text{osc}}(\omega)$  rapidly increases. It reaches its maximum around  $\omega_b$  and drops to a plateau with  $n_{\text{osc}}(\omega) \approx 8$ . This might at first sight look surprising, since the coupling between the oscillators, Eq. (22) was not changed. On closer inspection of the coupled equations of motion and the equilibrium condition, one sees, however, that the external force does in fact change the coupling between the single oscillators. The maximal value of  $n_{\text{osc}}(\omega)$  increases with  $f_{\text{ext}}^0$  opposite to  $g(\omega_b)/\omega_b^2$ . This is what one would intuitively expect from an increased coupling. As in the case of the DOS, also  $n_{\text{osc}}(\omega)$  depends on the original DOS,  $g_o(\omega)$ , for frequencies  $\omega > \omega_c > \omega_b$ .

### C. Distribution of anharmonicity parameters

So far, we have taken the anharmonicity parameter  $A$  in Eq. 7 as a constant and have neglected possible third order terms. To check the influence of distributions of these terms, we did additional simulations where we introduced distributions of these parameters. The scaled results are summarized in Fig. 6, where we also show for comparison the theoretical result of Eq. 11 (dotted line). The solid line gives the simulation results for  $g_o(\omega) \propto \omega^2$  and  $J = 0.2$  with a fixed value  $A = 1$ . The simulated BP is slightly wider than the theoretical prediction. The upturn at  $\omega/\omega_b \approx 2$  indicates the upper limit  $\omega_c$  where the interaction strength no longer suffices to destroy the assumed density of the non-interacting oscillators,  $g_o(\omega) \propto \omega^2$ . Taking, for the same parameters, random  $A_i$  from the interval  $[0.7, 1.3]$ , no significant change can be discerned. This is in agreement with our previous result<sup>3</sup> that this anharmonic term provides the mechanism to stabilize the interacting oscillators but, it's magnitude does not determine the resulting spectrum.

The situation is different when we add a third order term to the energy of the single oscillators, Eq. 7,

$$U_i(x) = Ax^4/4 + B_ix^3/3 + M\omega_i^2 x^2/2. \quad (25)$$

The dashed line in Fig. 6 shows the resulting BP for  $B_i = b_i\omega_i$  with  $b_i$  a random number from  $[-1, +1]$  ( $g_o(\omega) \propto \omega$ ). Compared to the curves without this term, the BP is considerably broadened even though it retains its general shape.

## VI. COMPARISON WITH EXPERIMENT

Unfortunately not too many experimental data are available. Our theory should, therefore, be considered rather as a prediction concerning future experiments than as an interpretation of the existing experimental data. A general increase of  $\omega_b$  has been observed in

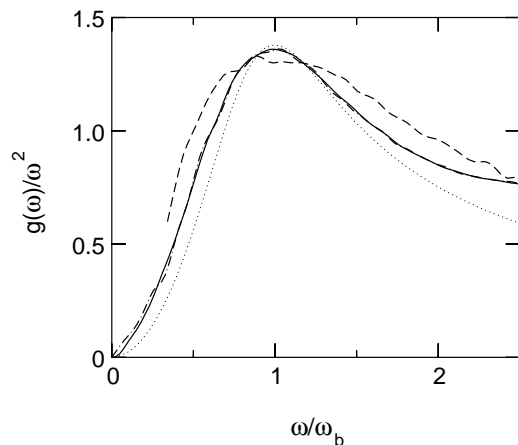


FIG. 6: Boson peak frequency,  $\omega_b$ , versus external force strength on a double logarithmic scale: crosses:  $N = 2197$ ,  $g_o(\omega) \propto \omega^2$ ,  $J = 0.1$ ; circles:  $N = 2197$ ,  $g_o(\omega) \propto \omega$ ,  $J = 0.07$ . The dashed lines give the fit with a Gaussian force distribution.

experiments on a number of materials, e.g.  $\text{SiO}_2$ <sup>25,26</sup>,  $\text{GeO}_2$ <sup>25</sup>,  $\text{GeS}_2$ <sup>27</sup>, polybutadiene<sup>28</sup>, polystyrene<sup>29</sup> and teflon<sup>30</sup>. Similar shifts have been reported from computer simulations of  $\text{SiO}_2$ <sup>31,32</sup>. However most of these data are not sufficient for a quantitative analysis.

The shift of the BP over a large pressure range has been measured in a- $\text{SiO}_2$ <sup>33</sup>. As shown in Fig. 7, the experimental data can be fitted by our theory using Eqs. (19) and (20) assuming a Lorentzian distribution [see Eq. (A3)]. The agreement between the theory and experiment remains good even for high pressures. Regarding very high pressures, our theory is applicable as long as the short range topology that determines the structure of QLV's does not change.

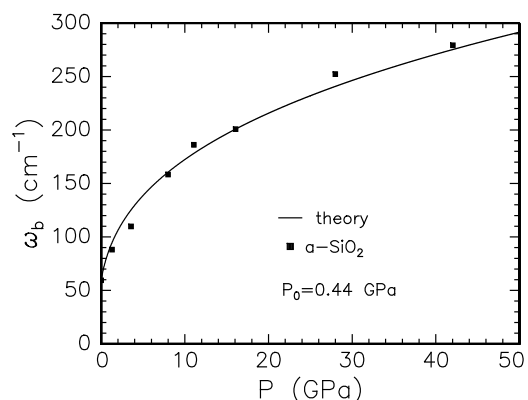


FIG. 7: The Boson peak in a- $\text{SiO}_2$  under pressure; filled squares are data of Ref. [33]

Fig. 8 shows the shift of the Boson peak in a- $\text{GeS}_2$  measured by Raman scattering. Although the scatter of the experimental points is rather large, again the general

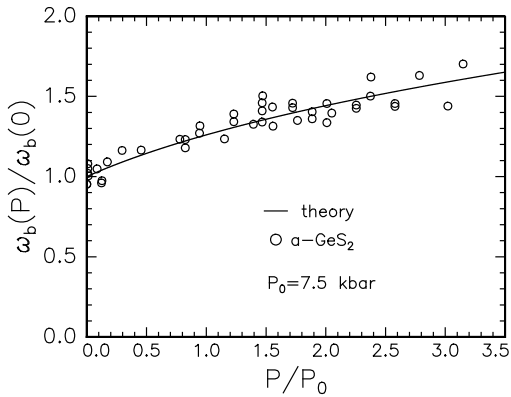


FIG. 8: The Boson peak in a-GeS<sub>2</sub> under pressure; open circles are data of Ref. [27]

agreement with our theory is encouraging.

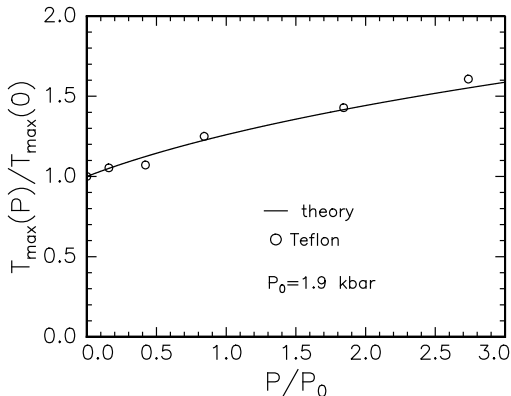


FIG. 9: The position of the bump  $T_{\max}(P)$  in the specific heat  $C(T)/T^3$  in teflon under pressure; open circles are the data of Ref. [30]

Boyer *et al.*<sup>30</sup> measured the shift with pressure of the low temperature maximum  $C(T)/T^3$  in Teflon, where  $C(T)$  is the specific heat. This maximum is directly related to the BP<sup>34</sup>. Again the observed shift fits well with our predictions, see Fig. 9.

However, the experiments on the change of the Boson peak position under pressure are so far insufficient. Therefore, we believe that further detailed investigations of this phenomenon are called for.

## VII. CONCLUSION

In our previous paper<sup>3</sup> we have proposed a mechanism of the Boson peak formation. The essence of the mechanism is that a vibrational instability of the spectrum of weakly interacting QLV is responsible for the origin of

the Boson peak in glasses and some other disordered systems. Anharmonicity stabilizes the structure but does not determine the shape of the Boson peak. The vibrations forming the Boson peak are harmonic.

The present paper extends these ideas. We show that under the action of hydrostatic pressure the Boson peak is shifted to higher frequencies. At comparatively low pressures the shift is linear in pressure  $P$  while for high pressures it is proportional to  $P^{1/3}$ . These conclusions are in good agreement with the existing experimental data. Our work explains the shift of the Boson peak without the need to postulate additional negative third order anharmonicities<sup>35</sup>.

To obtain a quantitative proof, more extensive investigations of the pressure dependence of the Boson peak position in various disordered systems are needed. Since the proposed mechanism is very general, it will also be interesting to investigate both theoretically and experimentally the behavior of the Boson peak under different types of strain other than the hydrostatic one, studied here, as well as under static electric fields. In future work, we hope to show that the same physical mechanism is fundamental not only for the formation of the Boson peak but also for such seemingly different phenomena as creation of the two level systems that dominate the properties of glasses at low temperatures.

## Acknowledgments

Two of the authors, VLG and DAP, gratefully acknowledge the financial support of the German Ministry of Science and Technology and the hospitality of the Forschungszentrum Jülich where part of the work was done. VLG also acknowledges the financial support of the Alexander von Humboldt Foundation and of the Russian Foundation for Basic Research under grant No 03-02-17638.

## APPENDIX A: CONVOLUTION

To make our investigation more general, we will consider Lorentzian and Gaussian distributions for both the random forces and the deformation potential. Besides, we will consider also a distribution of the deformation potential  $\Lambda$  that may be called “double Lorentzian”. This is formed by two superimposed Lorentzian distributions with widths  $\Lambda_0$  which are centered at  $\pm\lambda$ , respectively. For  $\lambda > \Lambda_0/\sqrt{3}$  the resulting distribution then has two symmetric side maxima and a minimum at  $\Lambda = 0$ .

For the Lorentzian distributions centered at zero one has

$$Q(f) = \frac{1}{\pi} \frac{f_0}{f^2 + f_0^2} = \frac{1}{2\pi} \int_{-\infty}^{\infty} d\tau_1 e^{if\tau_1 - f_0|\tau_1|}. \quad (\text{A1})$$

and

$$D(\Lambda) = \frac{1}{\pi} \frac{\Lambda_0}{\Lambda^2 + \Lambda_0^2} = \frac{1}{2\pi} \int_{-\infty}^{\infty} d\tau_2 e^{i\Lambda\tau_2 - \Lambda_0|\tau_2|}. \quad (\text{A2})$$

As a result of the convolution of these distributions one gets again a Lorentzian centered at zero but with greater width

$$F_P(f) = \frac{1}{\pi} \frac{\tilde{f}_0(P)}{f^2 + \tilde{f}_0^2(P)} \quad (\text{A3})$$

where

$$\tilde{f}_0(P) = f_0 + \frac{\Lambda_0|P|}{3K}. \quad (\text{A4})$$

In the same manner the convolution of two Gaussian distributions

$$Q(f) = \frac{1}{f_0\sqrt{2\pi}} e^{-f^2/2f_0^2} = \frac{1}{2\pi} \int_{-\infty}^{\infty} d\tau_1 e^{if\tau_1 - f_0^2\tau_1^2/2}, \quad (\text{A5})$$

and

$$D(\Lambda) = \frac{1}{\Lambda_0\sqrt{2\pi}} e^{-\Lambda^2/2\Lambda_0^2} = \frac{1}{2\pi} \int_{-\infty}^{\infty} d\tau_2 e^{i\Lambda\tau_2 - \Lambda_0^2\tau_2^2/2}, \quad (\text{A6})$$

leads to another Gaussian distribution with increased width:

$$F_P(f) = \frac{1}{\tilde{f}_0(P)\sqrt{2\pi}} \exp[-f^2/2\tilde{f}_0^2(P)] \quad (\text{A7})$$

where

$$\tilde{f}_0(P) = \sqrt{f_0^2 + \left(\frac{\Lambda_0 P}{3K}\right)^2}. \quad (\text{A8})$$

Finally let us convolute the Lorentzian for the internal forces, Eq. A1, with a double Lorentzian distribution:

$$D(\Lambda) = \frac{1}{2\pi} \left[ \frac{\Lambda_0}{(\Lambda - \lambda)^2 + \Lambda_0^2} + \frac{\Lambda_0}{(\Lambda + \lambda)^2 + \Lambda_0^2} \right]. \quad (\text{A9})$$

As a result of the convolution one gets

$$F_P(f) = \frac{\tilde{f}_0(P)}{2\pi} \left[ \frac{1}{(f + \alpha\lambda)^2 + \tilde{f}_0^2(P)} + \frac{1}{(f - \alpha\lambda)^2 + \tilde{f}_0^2(P)} \right] \quad (\text{A10})$$

where  $\alpha = P/3K$  and  $\tilde{f}_0(P)$  is given by Eq. (A4). This distribution now depends both on the widths of the two Lorentzians and on the distance between their centers,  $2\lambda$ , in  $D(\Lambda)$ .

- 
- <sup>1</sup> *Amorphous Solids. Low Temperature Properties*, edited by W. A. Phillips, (Springer-Verlag, Berlin:1981).
- <sup>2</sup> N. Ahmad, K. W. Hutt, W. A. Phillips, J. Phys. C: Solid State Phys. **19**, 3765 (1986).
- <sup>3</sup> V. L. Gurevich, D. A. Parshin and H. R. Schober, Phys. Rev. B **67**, 094203 (2003).
- <sup>4</sup> V. Gurarie and J. T. Chalker, Phys. Rev. Lett. **89**, 136801 (2002); Phys. Rev. B **68**, 134207 (2003).
- <sup>5</sup> W. Schirmacher, G. Diezemann, C. Ganter, Phys. Rev. Lett. **81**, 136 (1998).
- <sup>6</sup> T.S. Grigera, V. Martin-Mayor, G. Parisi, P. Verrocchio, J. Phys.: Cond. Matter **14**, 2167 (2002).
- <sup>7</sup> S.N.Taraskin, J.J.Ludlam, G.Natarajan, S.R.Elliott, Phil.Mag.B **82**, 197 (2002).
- <sup>8</sup> Y. Tezuka, S. Shin, M. Ishigame, Phys. Rev. Lett. **66**, 2356 (1991).
- <sup>9</sup> M. T. Dove, M. J. Harris, A. C. Hannon, J. M. Parker, I. P. Swainson, and M. Gambhir, Phys. Rev. Lett. **78** 1070 (1997).
- <sup>10</sup> V. N. Sigaev, E. N. Smelyanskaya, V. G. Plotnichenko, V. V. Koltashev, A. A. Volkov, and P. Pernice, J. Non-Cryst. Sol. **248**, 141 (1999).
- <sup>11</sup> M. A. Ramos, S. Vieira, F. J. Bermejo, J. Dawidowski, H. E. Fischer, H. Schöber, M. A. González, C. K. Loong, D. L. Price, Phys. Rev. Lett. **78**, 82 (1997).
- <sup>12</sup> R. M. Lynden-Bell, K. H. Michel, Rev. Mod. Phys. **66**, 721 (1994).
- <sup>13</sup> H. R. Schober, J. Phys.: Condens. Matter **16**, S2659 (2004).
- <sup>14</sup> W. Petry, G. Vogl, and W. Mansel, Z. Phys B **46**, 319 (1982).
- <sup>15</sup> H. R. Schober and G. Ruocco, Phil. Mag, **84**, 1361 (2004).
- <sup>16</sup> V. G. Karpov, M. I. Klinger, and F. N. Ignat'ev, Zh. Eksp. Teor. Fiz. **84**, 760 (1983) [Sov. Phys. JETP **57**, 439 (1983)].
- <sup>17</sup> M. A. Il'in, V. G. Karpov, D. A. Parshin, Sov. Phys. JETP **65**, 165 (1987).
- <sup>18</sup> U. Buchenau, Yu. M. Galperin, V. L. Gurevich, and H. R. Schober, Phys. Rev. B **43**, 5039 (1991).
- <sup>19</sup> B. B. Laird and H. R. Schober, Phys. Rev. Lett. **66**, 636 (1991); H. R. Schober and B. B. Laird, Phys. Rev. B **44**, 6746 (1991).
- <sup>20</sup> I. L. Aleiner and I. M. Ruzin, Phys. Rev. Lett. **72**, 1056 (1994).
- <sup>21</sup> M. M. Fogler Phys. Rev. Lett. **88**, 186402 (2002).
- <sup>22</sup> A. Heuer and R. J. Silbey, Phys. Rev. B **53**, 609 (1996).
- <sup>23</sup> H. R. Schober and C. Oligschleger, Phys. Rev. B **53**, 11469 (1996).
- <sup>24</sup> U. Buchenau, Yu. M. Galperin, V. L. Gurevich, D. A. Parshin, M. A. Ramos, H. R. Schober, Phys. Rev. B, **46**, 2798 (1992).
- <sup>25</sup> S. Sugai and A. Onodera, Phys. Rev. Lett. **77**, 4210 (1996).
- <sup>26</sup> Y. Inamura, M. Arai, M. Nakamura, T. Otomo, N. Kitamura, S. M. Bennington, A. C. Hannon, and U. Buchenau J.Non-Cryst.Sol. **293**, 389 (2001).



- <sup>27</sup> M. Yamaguchi, T. Nakayama, T. Yagi, *Physica B* **263-265**, 258 (1999).
- <sup>28</sup> B. Frick, C. Alba-Simionesco, *Appl. Phys. A* **74**, S549 (2002).
- <sup>29</sup> R. Geilenkeuser, Th. Porschberg, M. Jäckel, and A. Gladun, *Physica B* **263-264**, 276 (1999).
- <sup>30</sup> J. D. Boyer, J. C. Lasjaunias, R. A. Fisher, and N. E. Phillips, *J. Non-Cryst. Sol.* **55**, 413 (1983).
- <sup>31</sup> P. Jund and R. Jullien, *J. Chem. Phys.* **113**, 2768 (2000).
- <sup>32</sup> O. Pilla, L. Angelani, A. Fontana, J. R. Gonçalves, and G. Ruocco, *J. Phys.: Condens. Matter* **15**, S995 (2003).
- <sup>33</sup> R. J. Hemley, C. Meade, and H. Mao, *Phys. Rev. Lett.* **79**, 1420 (1997).
- <sup>34</sup> U. Buchenau, N. Nücker, A. J. Dianoux, N. Ahmad, and W. A. Phillips. *Phys. Rev. B* **34**, 5665 (1986).
- <sup>35</sup> V. Hizhnyakov, A. Laisaar, J. Kikas, An. Kuznetsov, V. Palm, and A. Suisalu, *Phys. Rev. B* **62**, 11296 (2000).